

Dynamic Analysis of Sand-Clay Layered Ground Considering a Viscous Effect of Clay

F. Oka & T. Kodaka

Department of Civil Engineering, Kyoto University, Sakyo-ku, Kyoto, JAPAN
foka@nakisuna.kuciv.kyoto-u.ac.jp, kodaka@nakisuna.kuciv.kyoto-u.ac.jp

Y.-S. Kim

Dam Safety Research Team, Water Resources Research Institute, Yuseong-gu, Daejeon, KOREA

Abstract: A cyclic viscoelastic-viscoplastic constitutive model for clay is incorporated into an effective stress based liquefaction analysis to describe viscous effect of clay layer to sand layer during earthquake. The seismic response against foreshocks, main shock as well as aftershocks of 1995 Hyogoken Nambu Earthquake is analyzed in the present study. Acceleration responses in both clay layer and just upper liquefiable sand layer are damped due to viscous effect of clay. In the case of main shock and the following aftershocks that occurred within less than 9 days after main event, acceleration responses near at ground surface are damped due to the developed excess pore water pressure, while that at ground surface are amplified in other cases. Using the viscoelastic-viscoplastic model for clay layer, time history of acceleration response in upper liquefiable sand layer can be well calculated, in particular in the range of microtremor process after main seismic motion.

1 INTRODUCTION

Since Niigata Earthquake in 1964, a large number of constitutive models for sand have been studied to describe the cyclic behavior and liquefaction of sands. Oka et al. (1999) also proposed a cyclic elasto-plastic model for sands based on nonlinear kinematic hardening rule. Considering that most of grounds in the Japanese water front are layered, effect of non-liquefiable clay layer to liquefiable sand layer is rather important to estimate the earthquake-resistant performance of the whole sand-clay layered ground. Oka (1992) developed a cyclic elasto-viscoplastic constitutive model for clay based on non-linear kinematic hardening rule. Although this model is suited to describe a cyclic behavior of clay for the range of middle to high level strain, viscous effect of clay for the range of low level strain could not be expressed by the elasto-viscoplastic model. From this reason we have developed a viscoelastic-viscoplastic model for clay, in which viscoelastic component is incorporated to the cyclic elasto-viscoplastic model, and we have shown that the viscoelastic-viscoplastic model could simulate the cyclic triaxial test of natural clay and strain level dependency of both shear modulus and hysteretic damping (Oka et al. 2001).

In the present study, the proposed viscoelastic-viscoplastic model for clay is installed to the effective stress based liquefaction analysis code, LIQCA-2D (Oka et al, 1994, 1999). Through the post analysis for foreshocks, main shock as well as aftershocks in Port Island, effect of clay layer laying beneath liquefiable sand layer to dynamic properties of the whole sand-clay layered ground is discussed, in particular during relatively small earthquake.

2 VISCOELASTIC-VISCOPLASTIC CONSTITUTIVE MODEL FOR CLAY

A cyclic viscoelastic-viscoplastic constitutive model proposed in the present study is formulated by incorporating a three-parameter viscoelastic component into an elasto-viscoplastic constitutive model based on non-linear kinematic hardening rule, which was proposed by Oka et al. (2002). The three-parameter viscoelastic

model, which combines a Voigt viscoelastic model and a linear elastic spring in series, has been used to describe a time-dependent behavior of clay for the range of low level strain by several researchers (i.e. Konder and Ho, 1965; Hori, 1974; Di Benedetto and Tatsuoka, 1997).

In the proposed model, the viscoelastic properties are considered only in the deviatoric strain rate component, because it is difficult to distinguish between the compressive viscoelastic behavior of soil skeleton and pseudo viscoelastic behavior due to the interaction of water and soil skeleton. The viscoelastic deviatoric strain rate tensor, \dot{e}_{ij}^{ve} , consists of an elastic deviatoric strain rate tensor, \dot{e}_{ij}^e , and a Voigt type viscoelastic deviatoric strain rate tensor, \dot{e}_{ij}^{vev} , as

$$\dot{e}_{ij}^{ve} = \dot{e}_{ij}^e + \dot{e}_{ij}^{vev} = \frac{1}{2G_1} \dot{s}_{ij} + \frac{1}{\mu} (s_{ij} - 2G_2 e_{ij}^{vev}) \quad (1)$$

where, s_{ij} and \dot{s}_{ij} are deviator stress tensor and deviator stress rate tensor, respectively. G_2 is an elastic shear modulus in the Voigt element and G_1 is the shear modulus of the other elastic spring, and μ is a viscous coefficient in the Voigt element. By adding an elastic volumetric strain rate and a viscoplastic strain rate tensor to \dot{e}_{ij}^{ve} in Eq.(1), the total strain rate tensor is given by

$$\dot{\epsilon}_{ij} = \dot{e}_{ij}^{ve} + \frac{1}{3} \dot{\epsilon}_v^e \delta_{ij} + \dot{\epsilon}_{ij}^{vp} = \dot{e}_{ij}^{ve} + \frac{\kappa}{3(1+e)} \frac{\dot{\sigma}'_m}{\sigma'_m} \delta_{ij} + \dot{\epsilon}_{ij}^{vp} \quad (2)$$

The viscoplastic strain rate tensor is expressed as follows (Oka, 1992; Oka et al., 2002):

$$\dot{\epsilon}_{ij}^{vp} = C_{01} \langle \Phi_1(f_y) \rangle \frac{\eta_{ij}^* - x_{ij}^*}{\bar{\eta}_x^*} + C_{02} \langle \Phi_1(f_y) \rangle \left\{ \bar{M}^* - \frac{\eta_{mn}^* (\eta_{mn}^* - x_{mn}^*)}{\bar{\eta}_x^*} \right\} \frac{\delta_{ij}}{3} \quad (3)$$

$$\bar{\eta}_x^* = \{ (\eta_{mn}^* - x_{mn}^*) (\eta_{mn}^* - x_{mn}^*) \}^{1/2}, \quad \eta_{ij}^* = s_{ij} / \sigma'_m$$

where, C_{01} and C_{02} are viscoplastic parameters, and MacCauley's bracket $\langle x \rangle$ expresses that $\langle x \rangle = x$, if $x > 0$, $\langle x \rangle = 0$, if $x \leq 0$.

The static yield function, f_y , and the viscoplastic parameters m' , Φ_1 are assumed as follows (Adachi and Oka, 1982):

$$\Phi_1(f_y) = \exp\{m' \cdot f_y\}, \quad f_y = \bar{\eta}_x^* = 0 \quad (4)$$

Referring to Chaboche and Rousselier (1980), the non-linear kinematical hardening parameter, x_{ij}^* , is defined by using the following evolutionary equation:

$$dx_{ij}^* = B_1(A_1 de_{ij}^{vp} - x_{ij}^* d\gamma^{vp}), \quad d\gamma^{vp} = (de_{ij}^{vp} de_{ij}^{vp})^{1/2} \quad (5)$$

where A_1 is related to the stress ratio at failure, namely $A_1 = M_f^*$, and B_1 is related to the viscoplastic shear modulus G^{vp} , namely $B_1 = G^{vp} / M_f^*$. B_1 is varied corresponding to the viscoplastic shear strain γ^{vp} ($= \int d\gamma^{vp}$) from initial value B_0 to the lower limit value B_s as follows:

$$B_1 = B_s + (B_0 - B_s) \exp(-B_t \gamma^{vp}) \quad (6)$$

where B_t is the decreasing rate of B_1 .

3 SEISMIC MOTION AMPLIFICATION CHARACTERISTICS IN PORT ISLAND

Fig.1 illustrates a soil profile in Port Island, where the heavy damage of civil structures occurred due to the 1995 Hyogoken Nambu Earthquake. The cyclic viscoelastic-viscoplastic model for clay layer is incorporated into the effective stress based liquefaction analysis code LIQCA-2D developed by Oka et al. (1994). For the sand layers, a cyclic elasto-plastic model proposed by Oka et al. (1999) is used. Foreshock-mainshock-aftershock sequence in Port Island was recorded by seismometer array as shown in Fig.1 and categorized to five groups as listed in Table 1. In the present study, the acceleration at G.L. -83 m was used as the input earthquake motion, and the seismic responses at various depths have been computed and compared to the records. We also compare between the analytical results by using the viscoelastic-viscoplastic model and the elasto-viscoplastic model for clay in order to estimate the viscoelastic effect of the clay layer for the range of low level strain. Soil parameters used in the analysis are listed in Table 2. Initial shear moduli were calculated from shear wave velocity measured in situ. Shear wave velocities in clay layer are listed in Table 3, which were back-analyzed from recorded seismic acceleration for each group (Furuta et al., 2000).

3.1 Amplification Ratio Distributions

The amplification ratio distributions of peak acceleration normalized by the value at GL.-83 m are represented in Fig.2,

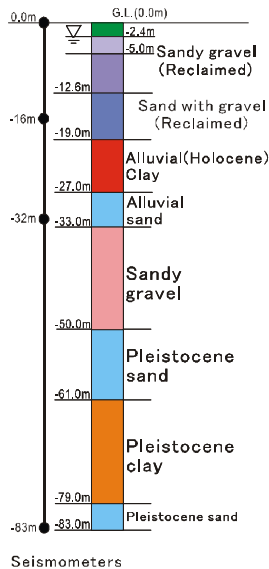


Fig.1. Soil profile in Port Island and schematic view of seismometer array

Table 1. Grouping of foreshocks, main shock and aftershocks

Group	Num. of earthquakes	Occurring date & time	Max. Acce. (gal)
A	5	1994/06/28 1:09pm ~1994/11/10 0:38am	9.9
Main shock	1	1995/01/17 5:46am	526.7
B	4	1995/01/17 5:53am ~1995/01/18 1:34pm	84.8
C	4	1995/01/19 1:00am ~1995/01/19 5:10am	19.3
D	10	1995/01/26 1:01am ~1995/02/24 8:03am	64.6
E	11	1995/03/05 10:04am ~1995/10/14 2:04am	84.6

Table 2. Soil parameters used in the present study

depth (-m)	0-2.4	2.4-5.0	5.0-12.6	12.6-19.0	19.0-27.0	27.0-33.0
soil type	sand	sand	sand	Sand	clay	sand
V_s (m/s)	170	170	210	210	Table 3	245
B_0	50000	10000	5000	5000	500	5000
B_s	1	1	1	1	1	1
B_t	1	1	1	1	1	1
M_m^*	0.71	0.71	0.75	0.75	0.74	0.91
M_f^*	1.01	1.01	1.05	1.05	1.24	1.21
λ	0.03	0.03	0.03	0.03	0.39	0.02
κ	0.00026	0.00027	0.00054	0.00072	0.05	0.00133
ν	0.25	0.25	0.25	0.25	0.488	0.25
e_0	0.6	0.6	0.6	0.6	1.5	0.6

Viscoelastic parameters for clay layer (G.L. 19.0-27.0m):
 $\mu=5.0E+03$ (kPa·sec), $C_{01}=2.0E-07$ (1/sec), $C_{02}=2.0E-09$ (1/sec), $m'_0=20$

Table 3. Back-analyzed shear wave velocities of clay layer (Furuta et al. 2000)

Time	Peak acc. at G.L. -83m (gal)		V_s (m/s)
	NS	EW	
1994/11/09 8:27pm	1.42	3.08	168.4
1995/01/17 5:46am	526.70	486.20	82.1
1995/01/17 8:58am	29.89	18.94	130.1
1995/01/25 11:16pm	—	—	—
1995/02/02 4:19pm	32.32	27.3	164.1
1995/02/12 3:17am	5.59	4.51	173.0

which shows measured records and numerical results by elastic-viscoplastic model (E-VP model) as well as viscoelasto-viscoplastic model (VE-VP model).

The characteristics of aftershock in Group D is very similar to that of foreshock in Group A. The results analyzed by the E-VP model show a great deal of amplification within the limit in the depth GL.-24 m ~ -40 m and near surface, while amplification is shown only near the surface in the results by VE-VP model. The de-amplification is shown within the limit at depth GL.-17 m ~ -24 m which includes the clay layer in the results by both models. It is clearly shown that the clay layer has damping effects toward the upper sand layer.

The point 'a' in the Main shock stands for the second peak data at -16 m. In the case of Main shock, the reason for the de-amplification is not only the effect of clay layer but also the effect of excess pore water pressure due to liquefaction. In particular, small amplification in near surface is totally different from the other groups except for the line 'b' in Group B.

The line 'b' and 'c' in Group B are the records of aftershock occurred about seven minutes and three hours after the main shock, respectively. The line 'b' is similar to the results of the main shock because of less time difference, while the others in Group B including the line 'c' are similar to Group A. Hence, it is revealed that during the 1995 Hyogoken Nambu Earthquake the excess pore water pressure was increased continually in the soil layer, in particular near the ground surface, and then it was almost recovered in 3 hours after the main shock, but not completely. Since the results of Group C are similar to that of Group B except the line 'b', the soil properties were probably not completely recovered yet. As mentioned above, the amplification ratio distribution during the

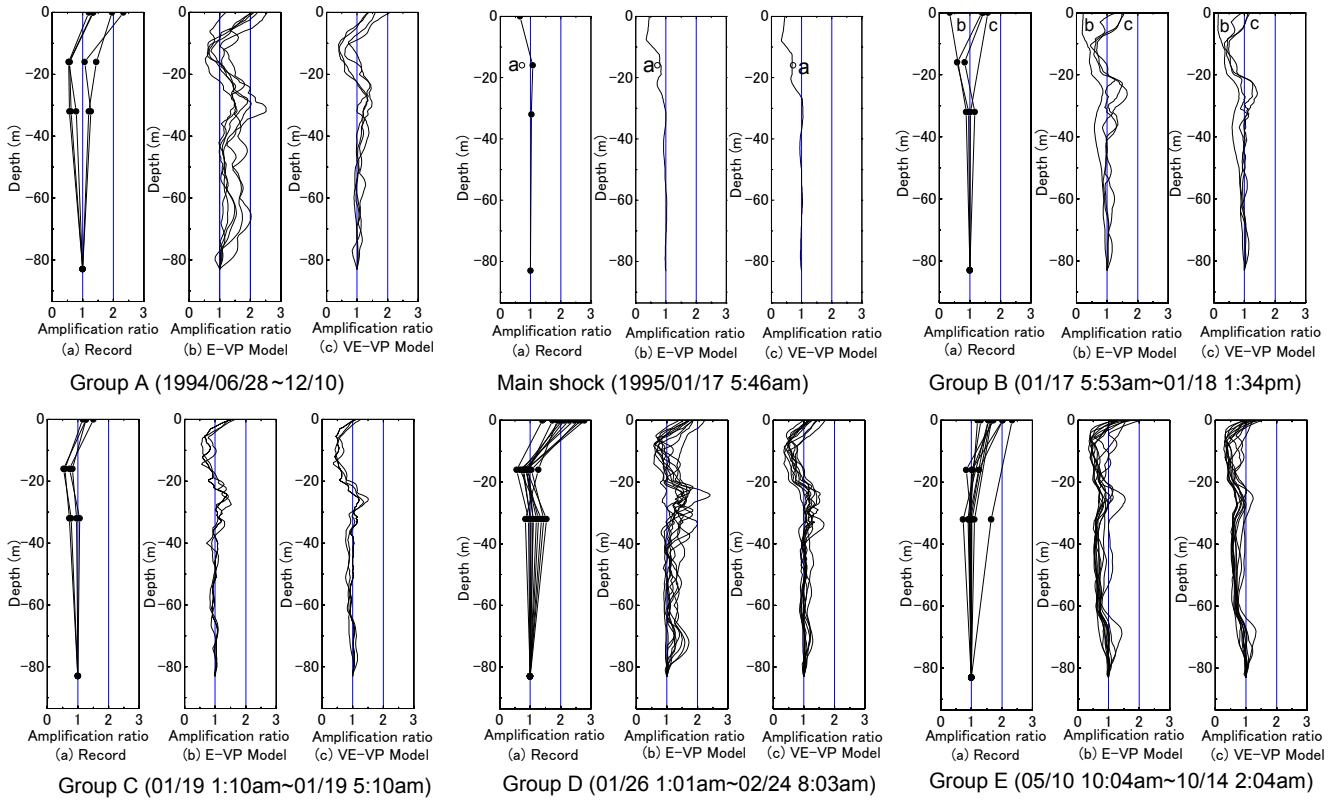


Fig.2. Amplification ratio distributions with depth (a) record, (b) analytical result by E-VP model, (c) analytical result by VE-VP model

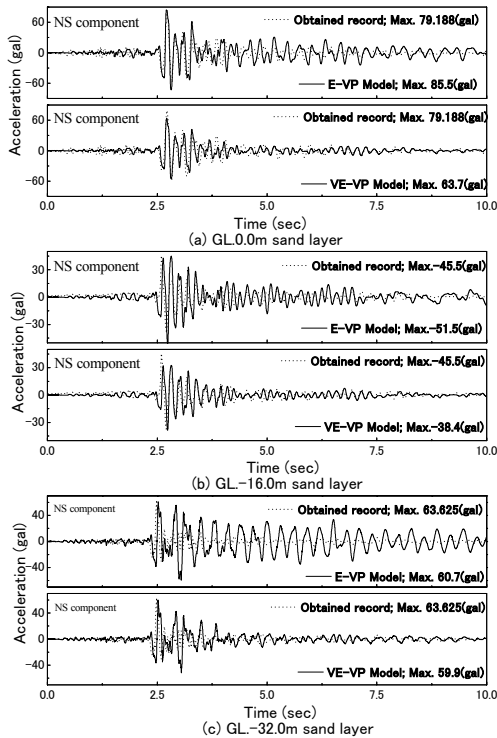


Fig.3. Time history of acceleration response (Group B)

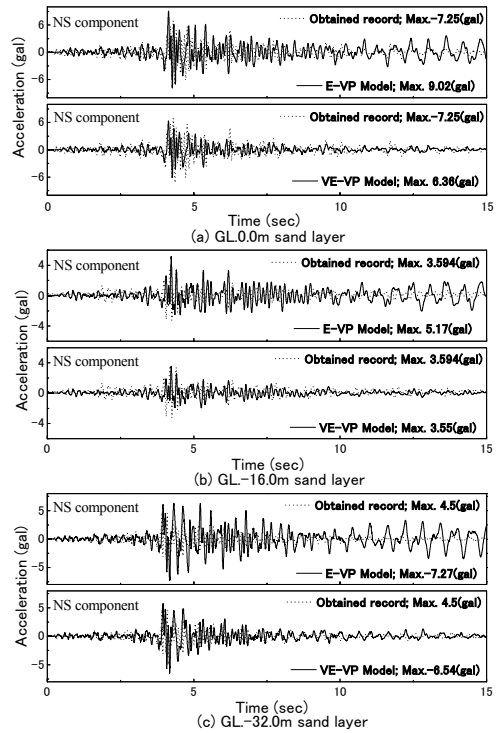


Fig.4. Time history of acceleration response (Group C)

aftershock of Group D is very similar to that of Group A, hence, the amplification of maximum acceleration is completely recovered. These results demonstrate that the dynamic soil characteristics can be recovered partly in three hours and completely in around nine days after the main shock.

3.2 Acceleration Response Analysis of Aftershocks

The representative earthquake record for each group is described herein. We compare the seismic responses calculated by both VE-VP and E-VP model with the obtained records during the aftershock to examine the model characteristics for the range of low

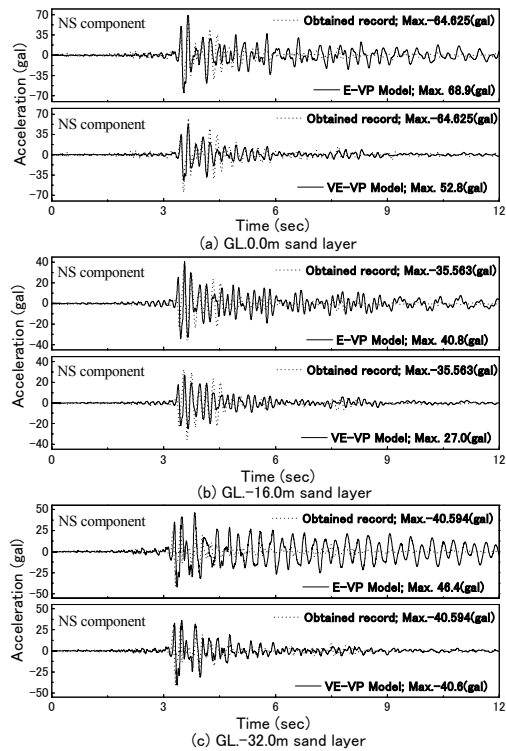


Fig.5. Time history of acceleration response (Group D)

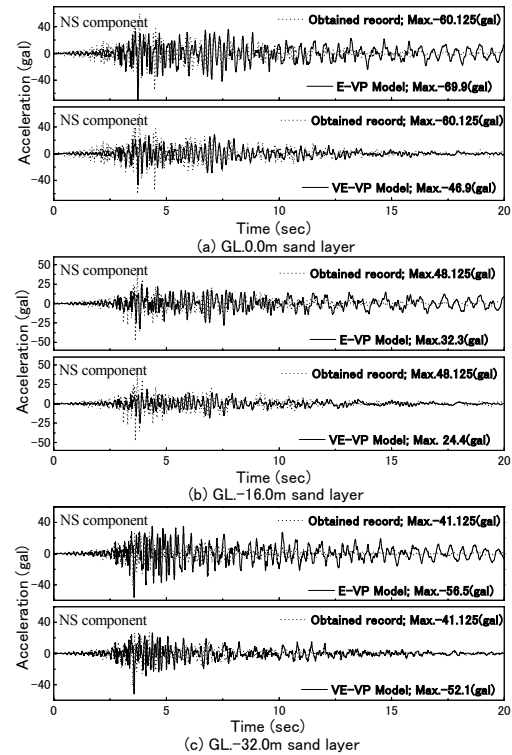


Fig.6. Time history of acceleration response (Group E)

level strain.

Fig.3 shows a time history of acceleration response of the aftershock occurred at 5:25am in 18th Jan. 1995 in Group B. The E-VP model shows larger acceleration response than the observed acceleration record for the range of low level strain; see for example between 4 seconds and 10 seconds in Fig.3. On the other hand, the VE-VP model well describes the time histories of acceleration for the range of low level strain. The comparison in smaller seismic motion is referred to the result in Group C. Fig.4 is acceleration response of the aftershock at 1:00am in 19th Jan., 1995 in Group C. The VE-VP model describes quite well the acceleration response while the E-VP model produces results, which do not match with the obtained records for the range of low level strain. Fig.5 presents the acceleration response of the earthquake at 4:19pm in 2nd Feb., 1995 in Group D. The peak acceleration at ground surface was about -65(gal). The VE-VP model gave results that matched well with obtained records, in particular in the small acceleration case. Fig.6 shows acceleration response of the aftershock at 2:04am in 14th Oct., 1995 in Group E and the maximum acceleration of obtained records at ground surface was about -60(gal). For this aftershock in Group E, the values of maximum acceleration at depths of -16m and 0.0m are smaller than the observed records. In particular, the VE-VP model underestimates the peak value of acceleration. On the other hand, as for the small strain range VE-VP model well reproduce the acceleration records after 7 seconds. This means that the VE-VP model describes well the time histories of acceleration, although VE-VP model rather underestimates the peak value of acceleration.

4 CONCLUSION

The amplification ratio distributions of acceleration were numerically analyzed by both the elasto-viscoplastic model and the viscoelastic-viscoplastic model for clay layer. The clay layer affects the upper sand layer as damping layer. In the case of main shock

and the following aftershocks that occurred within less than 9 days after main event, acceleration responses near at ground surface are damped due to the developed excess pore water pressure, while that at ground surface are amplified in other cases. The time history of acceleration response of the representative aftershock record for each group was also analyzed by two models for clay layer. The viscoelastic-viscoplastic model gave quite good overall description of the acceleration response for the whole layers, while the elastic-viscoplastic model produced results that did not match with the obtained records for the range of low level strain. This study reveals that the viscoelastic model can describe the damping characteristics of clay accurately for the range of low level strain, namely viscoelastic behavior, whereas the elastic-viscoplastic model cannot do so.

REFERENCES

- Adachi, T. & Oka, F. 1982. *Soils and Foundations*, 22 (4): 57-70.
- Chaboche, J.L. & Rousselier, G. 1983. *J. Pressure Vessel Tech., ASME*, 105: 103-158.
- Di Benedetto, H. & Tatsuoka, F. 1997. *Soils and Foundations*, 37(2): 127-138.
- Furuta, R. et al. 2000. *Proc. 4th Japan Conf. on Structural Safety and Reliability*: 289-296 (in Japanese).
- Hori, M. 1974. Fundamental studies on wave propagation characteristics through soils, *Ph.D. Dissertation, Dept. of Civil Engrg., Kyoto Univ.*: 90-143.
- Kondner, R.L. and Ho, M.M.K. 1965. *Transaction of the Society of Rheology*, 9(2): 329-342.
- Oka, F. 1992. *NUMOG IV*, 1: 105-114.
- Oka, F. et al. 1994. *Applied Scientific Research*, 52: 209-245.
- Oka, F. et al. 1999. *Geotechnique*, 49(5): 661-680.
- Oka, F. et al. 2002. *Int. J. Solids and Structures*, 39: 3625-3647.

